

ESTIMATION AND IDENTIFICATION OF PARAMETERS IN A LUMPED CEREBROVASCULAR MODEL

SCOTT R. POPE

Department of Mathematics, North Carolina State University
Campus Box 8205, Raleigh, NC 27695, USA

Laura M. Ellwein

Olin Engineering Center, Marquette University
1515 West Wisconsin Ave, Room 206, Milwaukee, WI 53233, USA

Cheryl L. Zapata

Department of Mathematics, University of Utah
155 S 1400 E, Salt Lake City, UT 84112, USA

Vera Novak

Harvard Medical School and Beth Israel Deaconess Medical Center Division of Gerontology
110 Francis Street LM0B Suite 1b, Boston, MA 02215, USA

C. T. Kelley and Mette S. Olufsen

Department of Mathematics, North Carolina State University
Campus Box 8205, Raleigh, NC 27695, USA

(Communicated by James F. Selgrade)

ABSTRACT. This study shows how sensitivity analysis and subset selection can be employed in a cardiovascular model to estimate total systemic resistance, cerebrovascular resistance, arterial compliance, and time for peak systolic ventricular pressure for healthy young and elderly subjects. These quantities are parameters in a simple lumped parameter model that predicts pressure and flow in the systemic circulation. The model is combined with experimental measurements of blood flow velocity from the middle cerebral artery and arterial finger blood pressure. To estimate the model parameters we use nonlinear optimization combined with sensitivity analysis and subset selection. Sensitivity analysis allows us to rank model parameters from the most to the least sensitive with respect to the output states (cerebral blood flow velocity and arterial blood pressure). Subset selection allows us to identify a set of independent candidate parameters that can be estimated given limited data. Analyses of output from both methods allow us to identify five independent sensitive parameters that can be estimated given the data. Results show that with the advance of age total systemic and cerebral resistances increase, that time for peak systolic ventricular pressure is increases, and that arterial compliance is reduced. Thus, the method discussed in this study provides a new methodology to extract clinical markers that cannot easily be assessed noninvasively.

2000 *Mathematics Subject Classification.* Primary: 92C30, 92C35, 92C50, 65L09; Secondary: 93B40.

Key words and phrases. cardiovascular modeling, systemic resistance, cerebrovascular resistance, parameter estimation, sensitivity analysis, subset selection.

1. **Introduction.** Cardiovascular system models have grown increasingly complex in recent years as more attempts are made to simulate physiological systems accurately. Examples of extensive models include the PNEUMA model developed by Fan and Khoo [9] and the cardio-respiratory model developed by Lu et al. [20]. Fan and Khoo combined cardiovascular, respiratory, and control models to simulate sleep apnea. The cardio-respiratory model by Lu et al. [20] was developed to predict the response to forced vital capacity and Valsalva maneuvers. Each of these models comprises more than one hundred differential equations and as many characterizing parameters. However, neither model has been validated against clinical data for the purpose of subject specific predictions. Combined with experimental data, such models can be used to estimate parameters (also known as biomarkers) that cannot be measured experimentally.

One approach to estimate model parameters is to use nonlinear optimization techniques that minimize the least squares residual between computed and measured quantities. For example, Olufsen et al. [28, 29] used the Nelder-Mead method [24] to predict parameters in a complex cardiovascular model developed to predict blood flow regulation during postural change from sitting to standing. In another study, Neal and Bassingthwaite [23] used a multi-step procedure for estimating subject-specific values for seventy-four parameters to examine cardiac output and total blood volume during hemorrhage.

The numerical optimization techniques used in this work necessitate some important considerations. First, any given set of optimal parameters only represents a local solution to the minimization problem: i.e., they only guarantee that a local minimum can be found. Parameters defining this local minimum may or may not be within physiological range, and there may be multiple sets of parameters that define the same model states. Thus, it is essential to compute initial, or “nominal,” parameter values using a priori knowledge such as height and weight, literature, or similar experiments. Second, the model output may be insensitive to some of the model parameters: i.e., a small change in some parameters may give rise to almost no change in the output states. It is not feasible to estimate insensitive parameters [7], either from a physiological or from a numerical perspective [18]. Furthermore, if any of the insensitive parameters are physiologically important, designing additional experiments may be necessary to estimate these parameters. Finally, model parameters may depend on each other. For example, given a mean flow through two resistance vessels, an infinite combination of resistances from each vessel could combine to give the same overall resistance; thus both parameters cannot be identified even though the model output will be sensitive to both parameters.

Some progress has been made toward stronger methodologies for parameter estimation. Ellwein et al. [7] used classical sensitivity analysis (as described by Es-lami [8] and Frank [10]) to rank parameters according to sensitivity. This ranking was used to separate parameters into two groups: one group consisted of parameters that the model output was sensitive to, and another group consisted of parameters that the model output was insensitive to. Ignoring the group of insensitive parameters gave rise to more reliable parameter estimates with a similar model output. In another study, Olansen et al. [27] used open-chest dog data combined with gradient-based optimization and sensitivity analysis to parameterize a cardiovascular model. For the latter study, the details of the chosen ranking algorithm were not revealed, and neither of these studies attempted to identify dependencies between model parameters. Other studies by Burth, Verghese and Velez-Reyes [5, 39] used a subset

selection algorithm to extract a set of independent parameters that can be estimated given a set of data (we define these parameters as identifiable). However, this study did not address the sensitivity of the model output to its parameters. In a more recent study, Heldt [14] combined sensitivity analysis and the subset selection method to identify a set of parameters that can be estimated reliably to predict quantities in a beat-to-beat cardiovascular system model.

In this study we have made additional progress toward using mathematical models to estimate key parameters given limited experimental data. To illustrate our method, we employ a simple five-compartment lumped parameter model that predicts cerebral blood flow velocity and arterial blood pressure in the systemic circulation during rest (in sitting position). Similar to previous work [7], we rank model parameters from the most to the least sensitive. In addition, we show how subset selection [5, 39] can be used to specify a subset of independent candidate parameters. Results from the sensitivity analysis and subset selection are combined to identify a final subset of independent and sensitive parameters that we estimate using a Gauss Newton gradient-based nonlinear optimization technique. This methodology (sensitivity analysis, subset selection, and optimization) is used to extract physiological biomarkers predicting systemic and cerebrovascular resistance, arterial compliance, and time for peak systolic ventricular pressure using pulsatile finger blood pressure and cerebral blood flow velocity data obtained non-invasively from twelve healthy young and twelve healthy elderly subjects.

2. Methods.

2.1. Experimental methods. Data to be analyzed in this study included non-invasive finger blood pressure and cerebral blood flow velocity measurements from twelve healthy young subjects aged 22-39 years (with a mean age of 28.8 ± 6.0 years) and twelve healthy elderly aged 56-74 years (with a mean age of 66.1 ± 6.4 years). Data were acquired in the Syncope and Falls in the Elderly (SAFE) laboratory at Beth Israel Deaconess Medical Center, Boston, and subjects provided informed consent signed by the Institutional Review Board at Beth Israel Deaconess Medical Center. The right and left middle cerebral arteries were insonated from the temporal windows with 2 MHz pulsed Doppler probes (MultiDop X4, DWL Neuroscan Inc. Sterling VA). Each probe was positioned to record the maximal flow velocities and stabilized using a three-dimensional head frame positioning system. Blood flow velocities were measured continuously in each of the middle cerebral arteries (see Fig. 1). In addition, peak-systolic, end-diastolic, and mean blood flow velocities were measured for each of the middle cerebral arteries. Blood pressure was recorded continuously from the index finger (see Fig. 1) using a Finapres device (Ohmeda Monitoring Systems, Englewood, CO) and blood pressure measurements were intermittently validated using tonography. To eliminate gravitational changes in blood pressure, the finger was kept at the level of the heart. The Finapres device provides reasonably accurate estimates of intra-arterial pressure if the finger position and temperature are kept constant [26]. The electrocardiogram was measured from a modified standard lead II using a Spacelab Monitor (SpaceLab Medical Inc., Issaquah, WA). Signals were recorded at 500 Hz using a Labview Data Acquisition System (NINDAQ) (National Instruments, Austin, TX). Measurements were obtained from subjects resting in a sitting position with their legs elevated at ninety degrees. Once a stable signal was obtained, data were recorded for five minutes.

From the steady sitting signal fifty cardiac cycles were extracted and stored (down-sampled to 50 Hz) for the offline model analysis.

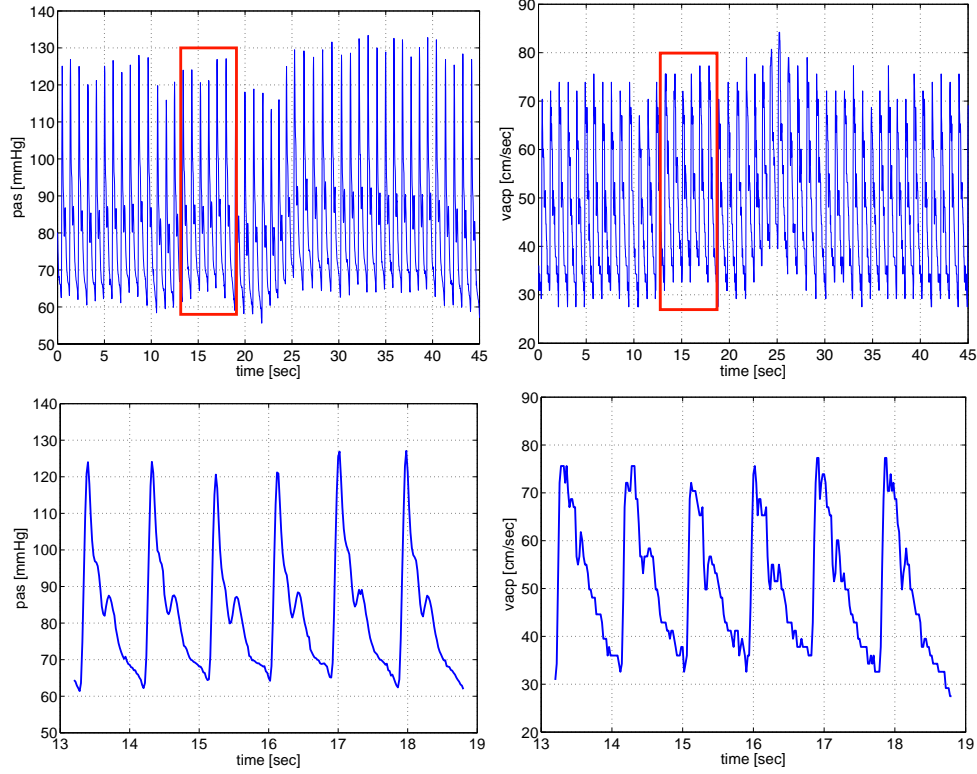


FIGURE 1. Arterial blood pressure (left) and cerebral blood flow velocity (right) from a healthy young subject. The top panel shows the entire time-series and the bottom panel shows a zoom over six seconds (areas zoomed are marked by boxes in the top panel).

2.2. Modeling and analysis.

2.2.1. *Basic cardiovascular model.* In this study we used a simple lumped parameter cardiovascular model of the systemic circulation similar to the model used in previous work [28, 29]. This model was originally developed to analyze cerebral blood flow velocity $v_{acp}(t)$ [cm/s] and finger blood pressure $p_{as}(t)$ [mmHg] measurements during orthostatic stress (sit-to-stand). In this study, the model was simplified to only account for dynamics during rest (sitting). Included in the current model are two arterial compartments and two venous compartments combining vessels in the body and the brain, as well as one heart compartment representing the left ventricle, Fig. 2. The left atrium was not modeled since previous studies [7] showed that parameters characterizing this compartment were insensitive. Furthermore, no experimental data were available predicting quantities in the pulmonary circulation.

The model uses a standard electrical circuit analogy in which the blood pressure difference $\Delta p = p(t) - p_0$ [mmHg] plays the role of voltage, the volumetric flow $q(t)$

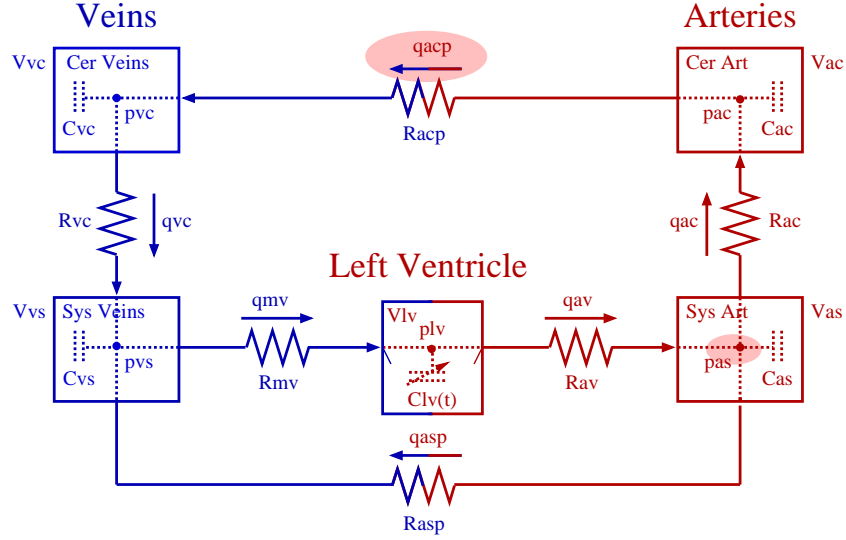


FIGURE 2. Electrical circuit representing arteries and veins in the systemic circulation, including the left ventricle “lv,” the systemic arteries “as,” the cerebral arteries “ac,” the cerebral veins “vc,” and the systemic veins “vs”. Each compartment contains a volume $V(t)$ [ml], a pressure $p(t)$ [mmHg], and a compliance (capacitor) C [ml/mmHg] (constant). Flow between compartments is marked by $q(t)$ [ml/s], and resistance to flow is marked by R [mmHg s/ml] (constant). The aortic and mitral valves are marked by small lines inside the left ventricle compartment. This model uses measurements of cerebral blood flow velocity $v_{acp}(t_j) = q_{acp}(t_j)/A_{acp}$ [ml/s], where A_{acp} [cm²] (constant) denotes the vessel area, and finger blood pressure $p_{as}(t)$ [mmHg]. These measurements are obtained at locations marked by gray ovals.

[ml/s] plays the role of current, and stressed volume $V(t)$ [ml] plays the role of electrical charge. For each compartment the stressed volume is defined as the difference between the total volume $V(t)$ and the unstressed volume V_{un} (constant). Compliance C [ml/mmHg] (constant) of the blood vessels is represented by capacitors, and resistors R [mmHg s/ml] (constant) are the same in both analogies. Similar to an electrical circuit, we define a pressure-volume relation of the form

$$V(t) = V_{un} + C(p(t) - p_0), \quad \text{where } p_0 = p_{atm}. \quad (1)$$

As shown in Fig. 2, all capacitors are linked to ground: i.e., pressures are relative to the exterior vascular pressure, set at the atmospheric pressure p_{atm} . Following Ohm’s law the flow between two compartments is defined by

$$q(t) = \frac{p_{in}(t) - p_{out}(t)}{R}. \quad (2)$$

Using these definitions, a differential equation for each of the arterial and venous compartments was derived by differentiating (1), while the equation for the heart compartment was obtained by imposing volume conservation. Thus the model can

be described by a system of five coupled ordinary differential equations with state variables $x(t) = [p_{as}(t), p_{ac}(t), p_{vs}(t), V_{lv}(t)]$, representing pressure in the systemic arteries $p_{as}(t)$, the cerebral arteries $p_{ac}(t)$, the systemic veins $p_{vs}(t)$, the cerebral veins $p_{vc}(t)$, and the left ventricular volume $V_{lv}(t)$. These are given by

$$\begin{aligned} \frac{dp_{as}(t)}{dt} &= \frac{1}{C_{as}} \left(\frac{p_{lv}(t) - p_{as}(t)}{R_{av}(t)} - \frac{p_{as}(t) - p_{vs}(t)}{R_{asp}} - \frac{p_{as}(t) - p_{ac}(t)}{R_{ac}} \right) \\ \frac{dp_{ac}(t)}{dt} &= \frac{1}{C_{ac}} \left(\frac{p_{as}(t) - p_{ac}(t)}{R_{ac}} - \frac{p_{ac}(t) - p_{vc}(t)}{R_{acp}} \right) \\ \frac{dp_{vs}(t)}{dt} &= \frac{1}{C_{vs}} \left(\frac{p_{as}(t) - p_{vs}(t)}{R_{asp}} + \frac{p_{vc}(t) - p_{vs}(t)}{R_{vc}} - \frac{p_{vs}(t) - p_{lv}(t)}{R_{mv}(t)} \right) \\ \frac{dp_{vc}(t)}{dt} &= \frac{1}{C_{vc}} \left(\frac{p_{ac}(t) - p_{vc}(t)}{R_{acp}} - \frac{p_{vc}(t) - p_{vs}(t)}{R_{vc}} \right) \\ \frac{dV_{lv}(t)}{dt} &= \frac{p_{vs}(t) - p_{lv}(t)}{R_{mv}(t)} - \frac{p_{lv}(t) - p_{as}(t)}{R_{av}(t)}, \end{aligned} \quad (3)$$

where the valve resistances $R_{mv}(t)$ and $R_{av}(t)$ are functions of time and the ventricular pressure $p_{lv}(t) = f(t, V_{lv}(t))$ is a function of the ventricular volume, as discussed in detail below.

To model the opening and closing of the valves, a piecewise continuous function representing the vessel resistance was developed, which define the “open” valve state using a small baseline resistance and the “closed” state using a value several magnitudes larger. This idea originally proposed by Rideout [36] and used in previous work [7, 28, 29] can be formulated using time varying resistances of the form

$$\begin{aligned} R_{mv}(t) &= \min(R_{mv,open} + \exp(-2(p_{vs}(t) - p_{lv}(t))), 10), \\ R_{av}(t) &= \min(R_{av,open} + \exp(-2(p_{lv}(t) - p_{as}(t))), 10). \end{aligned} \quad (4)$$

Following this equation, when $p_{lv}(t) < p_{vs}(t)$, blood flows into the ventricle and the mitral valve is open; as $p_{lv}(t)$ becomes greater than $p_{vs}(t)$, the resistance grows exponentially to a large constant value. We used the value ten; this value was chosen to ensure that there is practically no flow when the valve is closed. The value remains there for the duration of the closed valve phase. The transition from open to closed is not discrete; an exponential function is used for the partially opened valve, with the amount of “openness” given as a function of the pressure gradient. A smooth approximation was adapted from [6] to ensure that valve equations in (4) are differentiable, a necessary condition for the sensitivity analysis and the gradient-based optimization method [18]. Using the smooth approximation, the minimum in the valve equations (4) was computed as,

$$\min_{\epsilon}(x) = -\epsilon \ln \left(\sum_i \exp(-x_i/\epsilon) \right), \quad (5)$$

where $\epsilon > 0$ represents the degree of smoothness (large values of ϵ gives rise to more smoothing) and x represents the vector (indexed by i) to be minimized.

For the left ventricle, we predicted the change in volume using the differential equation,

$$\frac{dV_{lv}}{dt} = q_{vs} - q_{as},$$

while we used a simple elastance model defined by

$$p_{lv}(t) = E_{lv}(t) (V_{lv}(t) - V_d), \quad (6)$$

to predict ventricular pressure. In this model, $E_{lv}(t)$ [mmHg/ml] is the ventricular elastance; $V_{lv}(t)$ is the stressed ventricular volume; and V_d (constant) is the ventricular volume at zero diastolic pressure [31]. Note $V_{lv}(t)$ is computed using the volume conservation law in (3). No constraint was imposed to ensure that $V_{lv}(t) > V_d$. However, this did not pose any problems for our computations as shown in Fig. 6. To compute ventricular pressure we need only to prescribe an elastance function $E_{lv}(t)$. We modify a model developed by Heldt [15] to obtain

$$E_{lv}(t) = \begin{cases} E_m + \frac{E_M - E_m}{2} \left[1 - \cos\left(\frac{\pi}{T_M}\right) \right], & 0 \leq \tilde{t} \leq T_M \\ E_m + \frac{E_M - E_m}{2} \left[\cos\left(\frac{\pi}{T_r}(\tilde{t} - T_M)\right) + 1 \right], & T_M \leq \tilde{t} \leq T_M + T_r \\ E_M, & T_M + T_r \leq \tilde{t} < T. \end{cases}$$

The parameters T_M [s] and T_r [s] are functions of the cardiac cycle T [s], T_M being the time of peak elastance and T_r the remaining time for the start of diastolic relaxation. To estimate these parameters they are set up as fractions $T_{M,frac} = T_M/T$ and $T_{r,frac} = T_r/T$, where T [s] is the length of the cardiac cycle (obtained for each cardiac cycle using measurements of heart rate). Finally, we define E_m and E_M [mmHg/ml] as the minimum and maximum elastance values.

In summary, the model discussed above can be written as

$$\frac{dx}{dt} = f(t, x, \theta),$$

where $x(t) = [p_{as}(t), p_{ac}(t), p_{vs}(t), p_{vc}(t), V_{lv}(t)]$, represents the five states. This model has a total of sixteen parameters, including five heart parameters

$$\theta_{heart} = \{V_d, E_M, E_m, E_{M,frac}, T_{r,frac}\},$$

and ten cardiovascular parameters

$$\theta_{cardiovasc} = \{R_{av,open}, R_{asp}, R_{ac}, R_{acp}, R_{vc}, R_{mv,open}, C_{as}, C_{ac}, C_{vc}, C_{vs}\}.$$

We also include a scaling factor A_{acp} , which represents the combined cross-sectional area of the cerebral arteries. This factor relates the cerebral blood flow to the cerebral blood flow velocity, by $q_{acp}(t) = v_{acp}(t)A_{acp}$.

2.2.2. Model parameters. Initial values for the cardiovascular parameters (see Table 1), including those for the elastance heart model, can be found from physiological considerations. The initial iterates for E_m and E_M [mmHg/ml] are taken from Ottesen et al. [31]. Initial values for $T_{M,frac}$ and $T_{r,frac}$ were predicted using values given by Ottesen et al. [31] and Heldt [14].

Initial values for resistors and capacitors were determined separately for each subject studied. We defined the initial value for the peak systolic ventricular pressure as the peak of the experimentally predicted finger pressure. To allow blood flow down the pressure gradient, we defined initial values for systemic arterial pressure as 99.5% of the peak finger pressure and cerebral arterial pressure as 98% of the peak finger pressure. We have no information about venous pressures; thus we chose to set them based on standard physiological considerations (see e.g. [3, 13, 38]). We calculated total blood volume (in ml) as a function of body surface area, BSA (in m²) and gender [37] of the form

$$V_{tot} = \begin{cases} (3.29 \cdot BSA - 1.29) \cdot 1000, & \text{male} \\ (3.47 \cdot BSA - 1.954) \cdot 1000, & \text{female.} \end{cases} \quad (7)$$

TABLE 1. Initial values for all model parameters. In the second column, p_{max}^d [mmHg] is the maximum of the pressure data; the total volume V_{tot} [ml] is defined in (7), and the total flow $q_{tot} = V_{tot}/60$ [ml/s]. The parameter $A_{acp} = q_{acp}/v_{acp}$ [cm²] relates cerebral blood flow to cerebral blood flow velocity.

Pressure [mmHg]	$k \cdot p_{max}^d$ k	Flow [ml/s]	$k \cdot q_{tot}$ k	Resistances [mmHg s/ml]	Ohm's law
$p_{lv,sys}$	1.000	q_{av}	1.0	$R_{av,open}$	$(p_{lv,sys} - p_{as})/q_{av}$
p_{as}	0.995	q_{mv}	1.0	$R_{mv,open}$	$(p_{vs} - p_{lv,dia})/q_{mv}$
p_{ac}	0.980	q_{asp}	0.8	R_{asp}	$(p_{as} - p_{vs})/q_{asp}$
p_{vc}	10 [mmHg]	q_{ac}	0.2	R_{ac}	$(p_{as} - p_{ac})/q_{ac}$
p_{vs}	5 [mmHg]	q_{acp}	0.2	R_{acp}	$(p_{ac} - p_{vc})/q_{acp}$
$p_{lv,dia}$	2 [mmHg]	q_{vc}	0.2	R_{vc}	$(p_{vc} - p_{vs})/q_{vc}$
Volume [ml]	$k \cdot V_{tot}$ k	Capacitors [ml/mmHg]		Heart parameters E_i [mmHg s/ml], V_d [ml]	
V_{lv}	65 [ml]	C_{as}	$0.35 V_{as}/p_{as}$	$T_{M,frac}$	0.38
V_{as}	0.1094	C_{ac}	$0.35 V_{ac}/p_{ac}$	$T_{r,frac}$	0.18
V_{ac}	0.0193	C_{vs}	$0.08 V_{vs}/p_{vs}$	E_m	0.049
V_{vc}	0.0783	C_{vc}	$0.08 V_{vc}/p_{vc}$	E_M	2.49
V_{vs}	0.5634			V_d	10

To estimate BSA we used a relation originally proposed by Mosteller [21] and later reformulated by Reading and Freeman [35] on the form

$$BSA = \sqrt{\frac{w \cdot h}{3600}},$$

where w [kg] denotes the subjects weight and h [cm] is the subject's height. Based on the assumption that the systemic volume circulates in one minute [4] we determined the total systemic flow as $q_{tot} = V_{tot}/60$ [ml/s]. We further assumed that 20% of the flow goes to the brain, while 80% goes to the body: i.e., the systemic flow $q_{asp} = 0.8 \cdot q_{tot}$ and the cerebral flow $q_{ac} = q_{acp} = q_{vc} = 0.2 \cdot q_{tot}$. Note these quantities are time averaged. They will be used to determine nominal parameter values and initial values for the states. We define initial resistances using Ohm's law: i.e., $R_i = \Delta p/q_i$ [mmHg s/ml] where Δp denotes the pressure drop across the resistor R_i . Distribution of the total blood volume to each compartment is based on work by Beneken and DeWit [3], which gives both total volumes and estimates for the unstressed volume for each compartment. Based on these values initial iterates for each capacitor i are obtained using the pressure volume relation $C_i = (V_i - V_{un,i})/p_i$ [ml/mmHg].

2.2.3. *Parameter estimation.* The objective of this study is to identify a set of model parameters that in a reliable way can be estimated given measured values of arterial blood pressure $p_{as}(t)$, $j = 1, \dots, N$ and cerebral blood flow velocity $v_{acp}(t_j)$, $j = 1, \dots, N$, where N is the number of pressure and velocity observations, respectively. Data were analyzed for $M = 50$ cardiac cycles at a frequency of 50 Hz. To estimate these parameters we used nonlinear optimization minimizing the residual between computed and measured (noted by superscript d) pressure and velocities relative to

the measured quantities over all samples t_j . To this end we defined the vector y spanning both pressure and velocity: i.e., y has $2N$ entries, given by

$$y = [p_{as}(t_1), \dots, p_{as}(t_N), v_{acp}(t_1), \dots, v_{acp}(t_N)]^T. \quad (8)$$

To ensure that the model captures both the systolic values, noted by subscript ‘‘sys,’’ and the diastolic values, noted by subscript ‘‘dia,’’ of the pressure and velocity for each cardiac cycle, we defined additional vectors y_i , $i = sys, dia$ by

$$\begin{aligned} y_{sys} &= [p_{as,sys,1}, \dots, p_{as,sys,M}, v_{acp,sys,1}, \dots, v_{acp,sys,M}]^T, \\ y_{dia} &= [p_{as,dia,1}, \dots, p_{as,dia,M}, v_{acp,dia,1}, \dots, v_{acp,dia,M}]^T. \end{aligned}$$

To find systolic and diastolic values we computed the maximum (systolic) and minimum (diastolic) values of pressure and velocity for each cardiac cycle. To ensure that the functions are smooth we used the smoothing function in (5) to compute both systolic and diastolic values. Also note that each of these vectors concatenate pressure and velocity: i.e., each vector has $2M$ entries. These quantities do not depend on time, but represent the minimum (diastolic) and maximum (systolic) values for each cardiac cycle. Combining the vectors y , we defined the residual vector between computed (y_c) and measured (y_d) quantities as

$$\hat{R} = \begin{bmatrix} \frac{y_1^c - y_1^d}{\sqrt{N}y_1^d}, \dots, \frac{y_{2N}^c - y_{2N}^d}{\sqrt{N}y_{2N}^d}, \frac{y_{sys,1}^c - y_{sys,1}^d}{\sqrt{M}y_{sys,1}^d}, \dots, \frac{y_{sys,2M}^c - y_{sys,2M}^d}{\sqrt{M}y_{sys,2M}^d}, \\ \frac{y_{dia,1}^c - y_{dia,1}^d}{\sqrt{M}y_{dia,1}^d}, \dots, \frac{y_{dia,2M}^c - y_{dia,2M}^d}{\sqrt{M}y_{dia,2M}^d} \end{bmatrix}^T.$$

Since velocity and pressure have different units, and since components in this vector have different lengths, we scaled the residual by the value of the measurements and by the square root of the number of measurements (N, M , respectively). This definition of the residual vector \hat{R} gave rise to a least squares cost-function J of the form

$$\begin{aligned} J = \hat{R}^T \hat{R} = & \quad (9) \\ & \frac{1}{N} \sum_{i=1}^N \left| \frac{p_{as,i}^c - p_{as,i}^d}{p_{as,i}^d} \right| + \frac{1}{N} \sum_{i=1}^N \left| \frac{v_{acp,i}^c - v_{acp,i}^d}{v_{acp,i}^d} \right| + \\ & \frac{1}{M} \sum_{i=1}^M \left| \frac{p_{as,sys,i}^c - p_{as,sys,i}^d}{p_{as,sys,i}^d} \right| + \frac{1}{M} \sum_{i=1}^M \left| \frac{p_{as,dia,i}^c - p_{as,dia,i}^d}{p_{as,dia,i}^d} \right| + \\ & \frac{1}{M} \sum_{i=1}^M \left| \frac{v_{acp,sys,i}^c - v_{acp,sys,i}^d}{v_{acp,sys,i}^d} \right| + \frac{1}{M} \sum_{i=1}^M \left| \frac{v_{acp,dia,i}^c - v_{acp,dia,i}^d}{v_{acp,dia,i}^d} \right|. \end{aligned}$$

Instead of using optimization to estimate all model parameters, we employed a number of criteria discussed below to identify a limited set of parameters to be estimated. We used sensitivity analysis to rank parameters from the most to the least sensitive. Subsequently, we used subset selection to identify a limited number of independent candidate parameters. Combining results from both analyses allowed us to pick a set of parameters to be estimated for all healthy young and healthy elderly subjects. Finally, we used nonlinear optimization to estimate the parameters.

2.2.4. *Sensitivity analysis.* We define parameters whose change has a large impact on the model as “sensitive” and parameters whose change has a negligible affect on the model as “insensitive.” Attempting to identify insensitive parameters can cause poor behavior of optimization routines [18] and give rise to optimal values that are outside of physiological range. Similar to previous work by Ellwein et al. [7] we used classical sensitivity analysis to rank the model parameters from the most to the least sensitive.

Sensitivities are computed with respect to output vector y (8) that concatenates pressure and velocity evaluated at times of the measured observations t_j . Note that velocities $v_{acp}(t)$ (the second half of y) are not state variables in the differential equation model but are obtained by scaling the cerebrovascular flow $q_{acp}(t)$, found using Ohm’s law (2), with the total area A_{acp} (constant) of the cerebral vessels:

$$v_{acp}(t) = \frac{q_{acp}(t)}{A_{acp}} = \frac{p_{ac}(t) - p_{vc}(t)}{A_{acp}R_{acp}}. \quad (10)$$

Optimization methods (discussed below) are more efficient when all parameter values are of the same order of magnitude. The nominal parameter values for our model differ by three orders of magnitude (for example, $E_m \approx 0.05$, while $C_{vs} \approx 36$ initially). So, we rescaled the parameters by the natural logarithm: i.e., the model input to the optimizer is given by $\tilde{\theta} = \ln(\theta)$.

Using the scaled parameters, the relative (nondimensional) sensitivities $S_{i,k}$ of the output y_k to the i ’th parameter is defined by

$$S_{i,k} = \left. \frac{\partial y_k}{\partial \tilde{\theta}_i} \frac{\tilde{\theta}_i}{y_k} \right|_{\tilde{\theta}=\tilde{\theta}_0}, \quad \tilde{\theta}_i, y_k \neq 0.$$

Note, the length of $S_{i,k}$ is $2N$, since $S_{i,k}$ concatenates sensitivities of pressure and velocity with respect to each of the model parameters. As discussed in the model section, all model components are differentiable. We computed the derivative in the sensitivity equation using the forward difference approximation

$$\frac{\partial y_k}{\partial \tilde{\theta}_i} \approx \frac{y_k(t, \tilde{\theta} + h e_i) - y_k(t, \tilde{\theta})}{h},$$

where

$$e_i = \left[0 \dots 0 \overset{i}{\hat{1}} 0 \dots 0 \right]^T$$

is the unit vector in the i ’th component direction.

The forward difference approximation is less accurate than the analytic derivatives computed using automatic differentiation as proposed by Ellwein et al. [7] but is computationally faster and provides sufficient accuracy for our purposes. We used a scaled 2-norm to get the total sensitivity S_i to the i ’th parameter

$$S_i = \left(\frac{1}{2N} \sum_{k=1}^{2N} S_{i,k}^2 \right)^{1/2}.$$

The classical sensitivity analysis described above is a local analysis, and thus sensitivities depend on the values of the parameters. In this study the goal was to use sensitivity analysis to rank parameters in order of sensitivity and use this ranking in conjunction with results from subset selection to identify a set of parameters that

can be estimated for all subjects. This is done prior to actual parameter estimations; thus the sensitivity ranking was computed using nominal parameter values.

2.2.5. Subset selection. Attempting to optimize all parameters in the model can lead to unrealistic parameter estimates and poor optimizer performance, particularly if some of the model parameters are interdependent. To determine how many and which parameters can be identified reliably we implemented a modified version of the subset selection method (see Appendix for detail), originally proposed by Velez-Reyes [39] and discussed further by Burth et al. [5], and by Heldt [14].

The result of the subset selection process was a list of identifiable parameters and a list of parameters that should be held constant at nominal parameter values during the optimization process. To obtain physiologically relevant parameters, this method was carried out combined with expert knowledge of the system studied. For example, subset selection picked the scaling factor A_{acp} as an identifiable parameter, while the cerebrovascular resistance R_{acp} was grouped with parameters to be kept fixed. However, the parameter A_{acp} only appears once in the ODE system as a factor next to R_{acp} , while R_{acp} also appears inside one of the differential equations. Furthermore, R_{acp} is one of the biomarkers that we find important to estimate. Consequently, we fixed the parameter A_{acp} at its nominal and subsequently subset selection picked the parameter R_{acp} . Another observation was that for a healthy heart, the resistances associated with the heart valves $R_{mv,open}$ and $R_{av,open}$ should be small and should remain fixed in order to obtain a small pressure gradient at the time of peak blood flow [4]. However, in particular $R_{mv,open}$ is very sensitive, which makes sense: large valve resistances could indicate a blockage of the valve, and a large change in this parameter does have a significant impact on the model output. In this study we only analyzed data from healthy subjects; thus we evaluated sensitivities using nominal parameter values.

In summary, we used sensitivity analysis to rank parameters from the most to the least sensitive. Subsequently, we used subset selection and expert knowledge to predict independent candidate parameters. Results from both analyses were combined to find a limited set of independent and sensitive candidate parameters to be estimated for all subjects. To estimate these model parameters we used a trust-region variant of the gradient-based Gauss-Newton optimization method to minimize the cost J defined in (9). Gauss-Newton is an iterative method [18] that at each iteration uses a solution based on a local linear approximation to compute the next iterate. The theory supporting our method predicts convergence, even when the initial parameter estimates are far from the solution, and rapid convergence, when near the solution. We ran optimizations with the candidate parameters against a subset of our subjects and further adjusted the candidate list based on the performance of the optimizer.

3. Results. We analyzed data from twelve healthy subjects aged 22-39 years and twelve healthy elderly subjects aged 56-74 years with characteristics summarized in Table 2. Given initial values for model parameters we computed and ranked sensitivities for fifteen model parameters with respect to cerebral blood flow velocity $v_{acp}(t)$ and arterial blood pressure $p_{as}(t)$. An overall rank (see Fig. 3) was obtained from the average sensitivities across each group of subjects. As shown in Table 3, the output states ($v_{acp}(t)$ and $p_{as}(t)$) were also highly sensitive to initial values.

Subset selection was used to identify a set of independent candidate parameters. We repeated the subset selection for all datasets. It should be noted that subset

TABLE 2. Characteristics for both groups of subjects. For each group of subjects diastolic (D), systolic (S), and mean (M) velocities are followed by diastolic (D), systolic (S), and mean (M) pressures. Each row contains values obtained from the data (d) and the model (c). The top row gives the mean values computed as an average over all periods; the second row gives the corresponding standard deviation; and the last row gives the percent error obtained as the difference between measured and computed values relative to the measured values.

Young							Elderly						
	Velocity [cm/s]			Pressure [mmHg]				Velocity [cm/s]			Pressure [mmHg]		
	D	S	M	D	S	M		D	S	M	D	S	M
	Mean values							Mean values					
d	42	98	63	66	116	82	d	34	80	53	73	134	94
c	48	97	71	67	129	95	c	34	67	50	69	132	98
	Standard dev							Standard dev					
d	8.5	15	11	7.6	14	8.4	d	6.9	16	11	4.7	11	5.6
c	9.9	15	12	8.1	14	10	c	5.9	14	9.5	3.1	13	5.6
	% Error							% Error					
	14	4.2	13	2.8	11	16		4.2	17	4.1	6.2	4.0	4.6

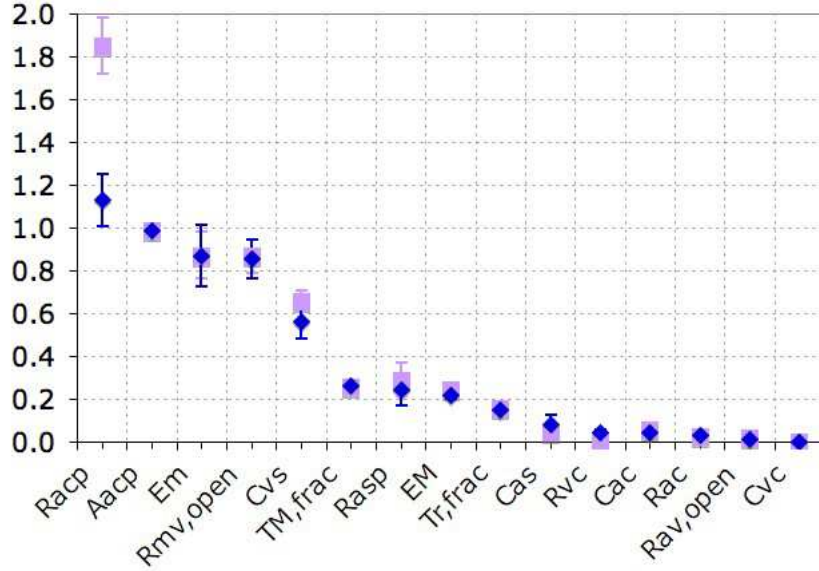


FIGURE 3. Overall ranking of the scaled model parameters $\ln(\theta)$ with one standard deviation for the healthy young subjects (dark marks) and healthy elderly subjects (light marks) ranked from the most to the least sensitive.

TABLE 3. Table of ranked sensitivities to initial conditions.

Parm	Sensitivity rank		Sensitivity rank	
	Young		Elderly	
$p_{as,0}$	1.87	1	1.78	1
$p_{vs,0}$	0.71	2	0.66	3
$V_{lv,0}$	0.62	3	0.98	2
$p_{ac,0}$	0.24	4	0.22	4
$p_{vc,0}$	0.14	5	0.13	5

selection does not depend on the output data; however, it is a local analysis: i.e., results will vary with the model parameters. For this study initial model parameters were predicted using morphometric information from each subject. In addition heart rate data were used as an input for each subject to determine the constant T (the length of each cardiac cycle), which is used in (6) to calculate left ventricular pressure. Results (see Fig. 4) showed that for both healthy young and healthy elderly subjects parameters R_{asp} , R_{acp} , C_{as} , $T_{M,frac}$, and E_M were picked for all subjects. In addition for the healthy young group, C_{ac} was picked once, while C_{vs} and E_m were picked twice. For the healthy elderly group, C_{ac} was picked for eleven subjects, C_{vs} was picked for eight subjects, and E_m was picked for three subjects. Four of the parameters chosen by subset selection for all subjects R_{asp} , R_{acp} , $T_{M,frac}$, and E_M were sensitive. Consequently, these parameters were included in the final set of parameters to be estimated for all subjects. The final parameter, picked for all subjects, was C_{as} , whose sensitivity is lower (see Fig. 3). For the elderly subjects two additional parameters were picked with high frequency: C_{ac} , which we didn't include since it is insensitive, and C_{vs} . C_{vs} has high sensitivity, and thus it should be included, but this parameter caused poor convergence of the optimizer; thus we left it out of the final set. Based on these observations the final set of parameters to be estimated for all subjects included R_{acp} , R_{asp} , $T_{M,frac}$, E_M , and C_{as} .

Optimized parameter values are summarized in Table 4. Results showed that R_{acp} , C_{as} (with a 10% confidence), and $T_{M,frac}$ differ between groups. This table also showed, as expected, that the total systemic resistance differs between the two groups. We computed a linear correlation factor (R^2 value) between computed and measured values of pressure and velocity. For young subjects overall correlation coefficients for pressure and velocity were 0.84 and 0.86, respectively. For the elderly subjects, the correlation was somewhat lower: 0.80 for blood pressure and 0.78 for blood flow velocity.

We also compared diastolic, systolic, and mean values for each signal. For the young subjects, the model gave rise to mean values that were approximately 15% higher than the corresponding measured values. This can be attributed to the fact that the model does not account for wave reflection. Note, our model does not include the dicrotic notch. The model also gave rise to systolic pressures and diastolic velocities that were approximately 12% too high, while the diastolic pressures and the systolic velocities were significantly more accurate, with less than 5% error. On the other hand, for the elderly subjects, the model did not systematically produce an overshoot or an undershoot. The systolic and diastolic values had a larger error, while the mean values were predicted more accurately. Even though these errors seem large, it should be noted that the model does not account for all demographic characteristics or for fluctuations due to respiration. Overall, the model predicts

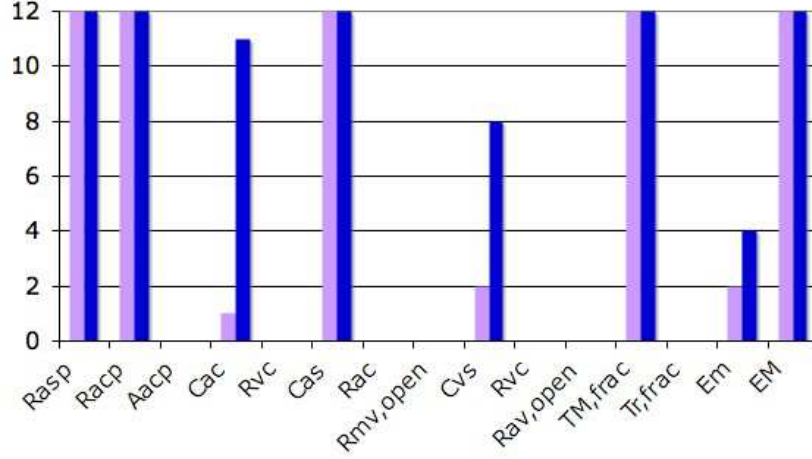


FIGURE 4. Frequencies of parameters from subset selection. Results for healthy young subjects are marked by dark bars, while results for healthy elderly subjects are marked by light bars. Note parameters R_{asp} , R_{acp} , C_{as} , $T_{M,frac}$, and E_M were picked for all datasets. In addition, for healthy young subjects, C_{ac} was picked once, while C_{vs} and E_m were picked twice. For the healthy elderly subjects, C_{ac} was picked for 11 subjects, C_{vs} was picked for eight subjects, and E_m was picked for three subjects.

the data well as shown in Fig. 5, which shows an example computation of $v_{acp}(t)$ and $p_{as}(t)$ using optimized parameters for a young subject. In addition Fig. 6 shows all internal states including ventricular pressure $p_{lv}(t)$ and volume $V_{lv}(t)$, systemic venous pressure $p_{vs}(t)$, and cerebral arterial $p_{ac}(t)$ and venous $p_{vc}(t)$ pressure. One limitation of our model is that it under-predicts cardiac output (not shown) by about 35%, and ventricular volume $V_{lv}(t)$ were shifted down toward lower values (see Fig. 6).

Another advantage of only identifying a limited number of parameters is that the computational efforts are significantly reduced. For most subjects, identification of five parameters required approximately ten iterations. These ten iterations lead to approximately sixty evaluations of the cost function (defined in (9)), one evaluation for each calculation of the cost function, and five additional evaluations used to calculate the finite difference Jacobian. The total computation time for the optimization was approximately eight hundred seconds (just over thirteen minutes) on a MacBook Pro 2.33 GHz laptop with 2 GB of memory running Matlab 7.4.

4. Discussion. This study showed that sensitivity analysis and subset selection enabled us to reliably identify five independent and sensitive parameters in a cardiovascular model, including a total of sixteen parameters. These results were obtained with a model that predicts cerebral blood flow velocity and arterial blood pressure using data from twelve healthy young and twelve healthy elderly subjects.

TABLE 4. Mean and standard deviation for initial and optimized values of the 5 identifiable parameters R_{asp} , R_{acp} , C_a , $T_{M,frac}$, and E_M . In addition, we have predicted the total resistance and compared that between young and elderly subjects. Since this is a derived parameter, no initial values are given. For each parameter the top row is obtained for the young subjects (marked by Y), while the bottom row denotes values obtained for the healthy elderly subjects (marked by E). The last column shows p-values comparing the optimized parameter values between healthy young and healthy elderly subjects.

Parm		Mean	Std	Mean	Std	p-value
		Initial parm		Optimized parm		
R_{asp}	Y	1.9	0.40	3.1	1.05	0.22
	E	2.0	0.32	3.8	1.38	
R_{acp}	Y	7.1	1.5	4.6	0.82	0.00
	E	17	3.2	6.4	1.57	
R_{tot}	Y	-	-	1.9	0.4	0.02
	E	-	-	2.5	0.7	
C_{as}	Y	1.5	0.30	0.53	0.15	0.07
	E	1.3	0.17	0.41	0.17	
$T_{M,frac}$	Y	0.38	0.00	0.12	0.015	0.00
	E	0.38	0.00	0.22	0.084	
E_M	Y	2.5	0.00	4.3	1.5	0.64
	E	2.5	0.00	4.0	1.7	

The five identifiable parameters were cerebrovascular resistance R_{acp} , systemic resistance R_{asp} , arterial compliance C_{as} , time for peak elastance relative to the length of the cardiac cycle $T_{M,frac}$, and maximum elastance E_M . During the optimization procedure these five parameters were identified, while all other parameters were kept fixed at their nominal parameter values.

The major advantage of limiting the number of parameters to be identified is that the parameter estimates become more reliable. For the twenty-four datasets analyzed in this study (twelve healthy young and twelve healthy elderly), reducing the number of parameters to be identified reduced the standard deviation for each parameter by several orders of magnitude. Furthermore, reducing the number of parameters to be optimized reduced the interdependency of the model parameters. For example, in this model, R_{acp} and A_{acp} are both sensitive (see Fig. 3), but they appear multiplied by each other in the calculation of cerebral blood flow velocity (10). Thus an infinite number of combinations of values for these two parameters could combine to give the same output states, preventing parameter values from being uniquely determined. Thus, we kept one of the two parameters (A_{acp}) constant, while we allowed the other parameter (R_{acp}) to fluctuate.

However, it is important to remember that the model does depend on the remaining eleven non-optimized parameters. Consequently, it becomes essential how these are calculated, since many of them vary by age, gender, height, mean pressure, etc. Nominal values for these non-optimized parameters were found as described previously.

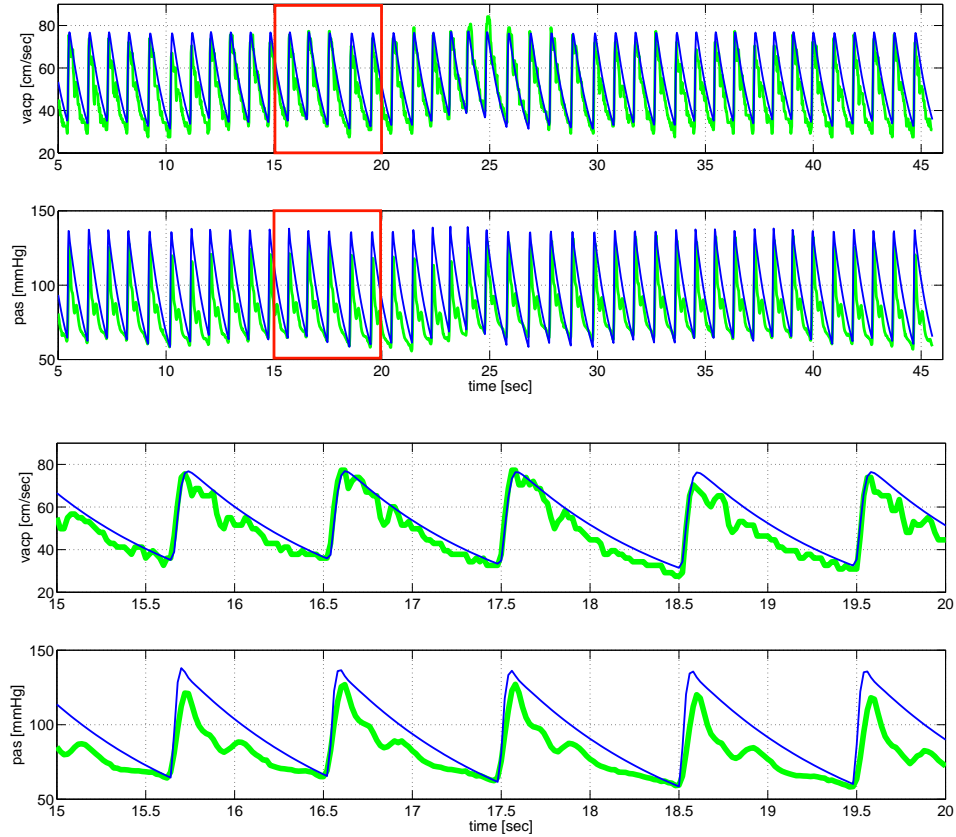


FIGURE 5. Experimental data (gray) and optimized (black) values for arterial pressure $p_{as}(t)$ and cerebral blood flow velocity $v_{acp}(t)$ for a healthy young subject. Top panel show results over the entire time-series, while the bottom panel shows a zoomed window from $15 < t < 20$ seconds.

A limitation of this study is that subset selection does not always pick the parameters that we find the most physiologically relevant. For example, subset selection often picked A_{acp} over R_{acp} . However, our goal was to predict R_{acp} . Thus, we chose to keep A_{acp} fixed at its nominal value while allowing R_{acp} to vary. With this additional constraint subset selection always picked R_{acp} as one of the parameters to be estimated. Another possibility would be to create a new parameter defined as the product of these two parameters. This composite parameter could then be compared between different groups of subjects, yet it would have less physiological accuracy than examining the parameters separately. Another advantage of a combined parameter is that we do not have to account for subject variation in total area A_{acp} . While transcranial Doppler studies by Aaslid and others [1, 19, 32] note that the cross-sectional area of the cerebral arteries is relatively constant over a

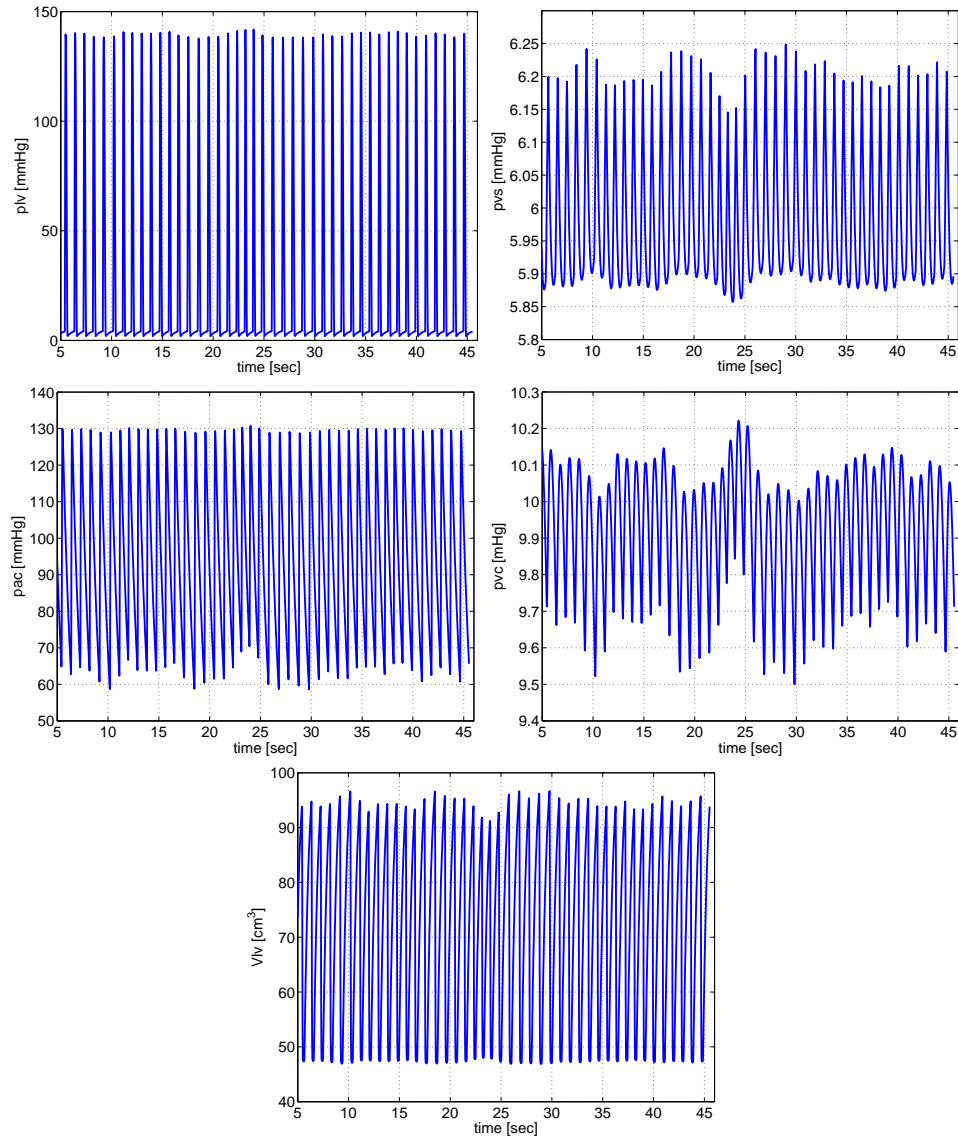


FIGURE 6. Additional model states including ventricular pressure $p_{lv}(t)$ and volume $V_{lv}(t)$, systemic venous pressure $p_{vs}(t)$, cerebral arterial pressure $p_{ac}(t)$, and cerebral venous pressure $p_{vc}(t)$. These results are shown for the same healthy subject used for computations depicted in Fig. 5.

wide range of mean flow velocities, the area do vary between subjects. Between-subject variation is not accounted for in this study, but A_{acp} could be determined

explicitly for each subject using vessel diameters measured on magnetic resonance angiographs.

With these modifications, subset selection picked the two major resistances R_{acp} and R_{aps} . Computations showed that R_{acp} varied significantly between groups of subjects, while R_{asp} did not. We did expect to find changes in R_{asp} . However, due to the simplicity of the cardiovascular model, and without any flow or velocity measurements for this portion of the system, we cannot make any conclusions on this part of the model. On the other hand, the total systemic resistance did show significant changes between the two groups of subjects. Classically, the total peripheral resistance is defined as the mean arterial pressure over cardiac output [2]. Given a mean pressure of 100 mmHg and an average cardiac output of 5 l/min (83.3 ml/s) the total resistance is 1.2 mmHg s/ml. Our results predicted R_{asp} as 1.9 mmHg s/ml for the healthy young subjects and 2.5 mmHg s/ml for the healthy elderly people. The model proposed here is validated against only cerebral blood flow velocity data and arterial blood pressure data. One limitation of our study was that, the model underestimated cardiac output. For most subjects cardiac output was calculated to be about 65% of a standard cardiac output, which led to higher values for the total resistance. One reason for our underestimation of cardiac output could be that the model does not include the left atrium, which plays the role of providing a preload for the left ventricle. However, results from our previous studies [7] showed that parameters characterizing this compartment were insensitive and that addition of the compartment did not significantly improve our results. Another reason could be that we have not accounted for the pulmonary circulation, which provides an additional reservoir for the system, a modification worth analyzing in future studies. Thus to ensure accurate cardiac output estimates we propose to either include measurements of cardiac output (which should be incorporated into the cost function) or to predict cardiac output from the blood pressure measurements, as suggested by Parlikar et al. [33], Wesseling et al. [41], and Mukkamala et al. [22].

Another traditional measure of resistance is the resistance index defined as the blood flow velocity pulse over the systolic velocity: i.e., $RI = (v_{acp}^{sys} - v_{acp}^{dia})/v_{acp}^{sys}$ [25, 34], and the pulsatility index defined as the blood flow velocity pulse over the mean blood flow velocity: i.e., $PI = (v_{acp}^{sys} - v_{acp}^{dia})/\bar{v}_{acp}$ [12, 25]. While these indices may be useful for detecting differences within a subject, we did not detect any differences between the two groups studied. For the healthy young subjects $RI^d = 0.51$ and $RI^c = 0.57$, while for the healthy elderly subjects $RI^d = 0.49$ and $RI^c = 0.58$. Similarly, for the healthy young subjects the pulsatility indices were $PI^d = 0.69$ and $PI^c = 0.89$, while for the healthy elderly subjects $PI^d = 0.66$ and $PI^c = 0.87$. For all indices superscript d denotes that the quantity is obtained from measurements and c denotes that the quantity is extracted from the model.

Another observation was that subset selection picked C_{as} (systemic arterial compliance) rather than C_{vs} (systemic venous compliance), which is more sensitive (see Table 3). From a physiological viewpoint C_{vs} may be more significant; however, C_{as} is significantly closer to the data collection site (finger arterial pressure); thus this parameter likely plays a larger role in predicting the pressure data. To investigate this further, we suggest testing if subset selection would pick C_{vs} if C_{as} is kept fixed at its nominal parameter value.

We also observed that $R_{mv,open}$ was very sensitive, but physically, we know that all subjects had well functioning heart valves. Consequently, this parameter should remain small and not be optimized. In fact, subset selection did initially pick this

parameter. However, optimizing it caused computed ventricular pressures to be outside of the physiological range. On the other hand, $R_{av,open}$ had a low sensitivity and was never picked; thus we did not have to include special considerations for this parameter.

Finally, we observed that for the healthy elderly subjects, subset selection picked seven parameters rather than five. The two additional parameters included C_{ac} , which is highly insensitive, and C_{vs} . To study the effect of this difference, we ran simulations for the elderly optimizing all seven parameters. Including both additional parameters led to poor performance of the optimizer. This is predictable since we included an insensitive parameter (C_{ac}), which cannot easily be estimated given the data. Including six parameters (i.e., adding the parameter C_{vs}) also led to poor performance of the optimizer. This cannot be explained by insensitivity, but may be related to parameter dependencies not captured by the subset-selection algorithm. More research into this will be done in future work.

Regarding the heart parameters, subset selection identified two parameters: time for maximum elastance relative to the length of the cardiac cycle ($T_{M,frac}$) and the maximum elastance (E_M). The parameter $T_{M,frac}$ differed significantly between the two groups of subjects, while no statistical significance was observed for E_M . The larger $T_{M,frac}$ value found in the elderly subjects can be explained by accounting for wave-reflection as described by Vlachopoulos and O'Rourke [40]. In elderly people, stiffer arteries cause the reflected pressure wave to augment the forward wave coming from the ventricle in late systole. This appears as a peak in the aortic pressure waveform that occurs later than and partially masks the systolic peak. Since the sole generator of the arterial waveform in our model is the ventricular pressure function, it is natural that this feature observed in elderly subjects appears in the $T_{M,frac}$ parameter.

It should be noted again, that this study included a simple heart model, which may not capture as many physiological attributes as other more detailed models, such as the fourteen parameter model developed by Ottesen and Danielsen [30]. A nice feature that we found (not shown) is that if one replaces the simple four parameter heart model with Ottesen and Danielsens fourteen parameter heart model, subset selection still identifies the same three cardiovascular parameters in addition to three heart parameters.

Mathematical models studied in the last decade have tended to be large comprehensive models with many states and parameters. Modelers often praise these models for their complexity and biological relevance, while experimentalists criticize the same models for being of little use for prediction. One of the main problems is that it is not possible to identify model parameters and compare these over large datasets. Standard deviations in parameters are large, in particular because such models often contain insensitive and interdependent parameters that hamper parameter identification and optimization. In this study, we have shown that subset selection and sensitivity analysis combined with measurements of cerebral blood flow velocity and arterial blood pressure can be used to identify five model parameters. Having a limited number of parameters allowed us to identify two biomarkers that vary between healthy young and elderly subjects: our modeling revealed, as expected, that cerebrovascular resistance and time for peak elastance was higher in healthy aging. While these physiological results are not new, they show that the proposed parameter identification methodology has potential to be applied to clinical studies. In future work we plan to use this methodology to predict biomarkers in

more comprehensive models such as the blood flow and pressure regulation model developed by Olufsen et al. [28, 29].

Acknowledgements. This research was supported in part by the National Science Foundation under grant NSF/DMS-0616597 (PI, Olufsen), NSF/DMS-0707220 and NSF/DMS-0404537 (PI, Kelley). Experimental efforts were supported by the American Diabetes Association, under grants 1-03-CR-23 and 1-06-CR-25 (PI, Novak), and the National Institute of Health under grant NIH/NINDS 1R01-NS045745-01A2 (PI, Novak), and from a general clinical research center grant MO1-RR01032 (PI, Novak). Scott Pope was partially supported by NIH-NIA (1 T32 AG023480-04). Authors would also like to acknowledge the NCSU IT for allowing us to use their linux cluster for computations. Finally, authors would like to thank Thomas Heldt, Laboratory for Electromagnetic and Electronic Systems, Massachusetts Institute of Technology, Boston, MA.

Appendix. Subset selection analyzes the Jacobian matrix ($R' = dR/d\tilde{\theta}$) computed from the scaled residual vector R . The entry at row i and column j of the Jacobian is $\partial R_i/\partial \tilde{\theta}_j$. Using the Jacobian, singular value decomposition $R' = U\Sigma V^T$ is used to obtain a numerical rank for R' . This numerical rank is then used to determine ρ parameters that can be identified given the model output y defined in (8). QR decomposition is used to determine the ρ identifiable parameters to which our system is sensitive as *a group*. This differs from sensitivity analysis, which finds parameters to which our system is *individually* sensitive. The subset selection algorithm presented here is similar to the one used in [5, 14]. Our method differs in our determination of the number of identifiable parameters. Previous methods look for large gaps in the eigenvalues of the model Hessian. In our problem such gaps do not exist, so we use an error estimate in our computation of the Jacobian as a lower bound on acceptable singular values.

Subset selection algorithm:

1. Given an initial parameter estimate, $\tilde{\theta}_0$, compute the Jacobian, $R'(\tilde{\theta}_0)$ and the singular value decomposition $R' = U\Sigma V^T$, where Σ is a diagonal matrix containing the singular values of R' in decreasing order, and V is an orthogonal matrix of right singular vectors.
2. Determine ρ , the numerical rank of R' . This can be done by determining a smallest allowable singular value.
3. Partition the matrix of eigenvectors in the form $V = [V_\rho V_{n-\rho}]$.
4. Determine a permutation matrix P by constructing a QR decomposition with column pivoting, see [11] p. 235, for V_ρ^T . That is, determine P such that

$$V_\rho^T P = QR,$$

where Q is an orthogonal matrix and the first ρ columns of R form an upper triangular matrix with diagonal elements in decreasing order.

5. Use P to re-order the parameter vector $\tilde{\theta}_0$ according to $\hat{\tilde{\theta}}_0 = P^T \tilde{\theta}_0$.
6. Make the partition $\hat{\tilde{\theta}}_0 = [\hat{\tilde{\theta}}_{0,\rho} \hat{\tilde{\theta}}_{0,n-\rho}]$ where $\hat{\tilde{\theta}}_{0,\rho}$ contains the first ρ elements of $\hat{\tilde{\theta}}_0$. Fix $\hat{\tilde{\theta}}_{n-\rho}$ at the a priori estimate $\hat{\tilde{\theta}}_{0,n-\rho}$.
7. Compute the new estimate of the parameter vector $\hat{\tilde{\theta}}$ by solving the reduced-order minimization problem

$$\hat{\tilde{\theta}} = \arg \min_{\tilde{\theta}} J(\tilde{\theta}), \quad \text{with } \hat{\tilde{\theta}}_{n-\rho} \text{ fixed at nominal values } \hat{\tilde{\theta}}_{0,n-\rho}.$$

Steps one and two are used to determine the numerical rank ρ of R' . The smallest singular value can be found by analyzing the Jacobian error bound. Since the Jacobian is computed using forward differences, the error of the Jacobian is approximately the square root of the error tolerance of the ODE solver. Thus if ϵ_S is the Jacobian error, then, according to [11] p. 428, this error can change the singular values of the Jacobian by ϵ_S . Thus, we cannot trust any singular value smaller than ϵ_S , and consequently, we use ϵ_S as the smallest acceptable singular value. In this study we used Matlabs differential equations solver ODE15S with an absolute error tolerance of 10^{-6} : i.e., the error of the numerical model solution is of order 10^{-6} and the error in the Jacobian matrix is approximately $\sqrt{10^{-6}} = 10^{-3}$. Consequently, singular values should not be smaller than 10^{-3} . Since the error of the Jacobian is an approximation, the smallest singular value that we accept is 10^{-2} . If errors are relative instead of absolute, the smallest acceptable singular values are $10^{-2}\|R'\|_2$. The latter condition is equivalent to choosing columns of R' that form a matrix with condition number no greater than 10^2 .

Once the number of identifiable parameters has been determined, we find the most dominant parameters by performing a QR decomposition with column pivoting on the most dominant right singular vectors computed in step 4. The process begins by choosing the most sensitive parameter in a way similar but not identical to the sensitivity analysis of the previous section; the column with largest 2-norm is chosen. The algorithm chooses additional parameters in a way that keeps the condition number of the chosen columns small; for more detail see [11] p. 233–36.

REFERENCES

- [1] R. Aaslid, K-F Lindegaard, W. Sorteberg and H. Nornes, *Cerebral autoregulation dynamics in humans*, *Stroke*, **20** (1989), 45–52.
- [2] F. Aletti, E. Lanzarone, M. Costantino and G. Baselli, *Non-linear modulation of total peripheral resistance due to pulsatility: a model study*, *Comp Cardiol*, **33** (2006), 653–56.
- [3] J. Beneken and B. DeWit, *A physical approach to hemodynamic aspects of the human cardiovascular system* in “Physical Bases of Circulatory Transport: Regulation and Exchange” (eds. E. Reeve and A. Guyton), W. B. Saunders, Philadelphia, PA, (1967), 1–45.
- [4] W. Boron and E. Boulpaep, “Medical Physiology,” W. B. Saunders, Philadelphia, PA, 2003.
- [5] M. Burth, G. Verghese and M. Valerez-Reyes, *Subset selection for improved parameter estimation in on-line identification of a synchronous generator*, *IEEE Trans Power Systems*, **14** (1999), 218–25.
- [6] X. Chen, L. Qi and K-L. Teo, *Smooth convex approximation to the maximum eigenvalue function*, *J Global Opt*, **30** (2004), 253–70.
- [7] L. Ellwein, H. T. Tran, C. Zapata, V. Novak and M. S. Olufsen, *Sensitivity analysis and model assessment: Mathematical models for arterial blood flow and blood pressure*, *J Cardiovasc Eng*, **8** (2008), 94–108.
- [8] M. Eslami, “Theory of Sensitivity in Dynamic Systems: an Introduction,” Springer Verlag, Berlin, Germany, 1994.
- [9] H-H. Fan and M. Khoo, *PNEUMA a comprehensive cardiorespiratory model*, *Eng Med Biol*, 2nd Joint EMBS/BMES Conference (2002), 1533–34.
- [10] P. Frank “Introduction to Sensitivity Theory,” Academic Press, New York, NY, 1978.
- [11] G. Golub and C. Van Loan, “Matrix Computations,” The Johns Hopkins Univ Press, Baltimore, MD, 1989.
- [12] R. Gosling and D. King, *Arterial assessment by Doppler shift ultrasound*, *Proc R Soc Med*, **67** (1974), 447–49.
- [13] A. Guyton and J. Hall, “Textbook of Medical Physiology,” W. B. Saunders, Philadelphia, PA, 1996.

- [14] T. Heldt, “Computational Models of Cardiovascular Response to Orthostatic Stress,” Ph.D. Thesis, Harvard/MIT Division of Health Science and Technology, MIT, 2004.
- [15] T. Heldt, E. Shim, R. Kamm and R. Mark, *Computational modeling of cardiovascular response to orthostatic stress*, J Appl Physiol, **92** (2002), 1239–54.
- [16] J. Hindalgo, S. Nadler and T. Bloch, *The use of the electroic digital computer to determine best fit of blood volume formulas*, J Nuclear Med, **3** (1962), 94–99.
- [17] C. T. Kelley, “Iterative Methods for Linear and Nonlinear Equations,” SIAM, Philadelphia, PA, 1995.
- [18] C. T. Kelley, “Iterative Methods for Optimization,” SIAM, Philadelphia, PA, 1999.
- [19] D. S. Kimmerly, E. Tutungi, T. D. Wilson, J. M. Serrador, A. W. Gelb, R. L. Hughson and J. Shoemaker, *Circulation norepinephrine and cerebrovascular control in conscious humans*, Clin Physiol Funct Imag, **23** (2003), 314–19.
- [20] K. Lu, J. Clark, F. Ghorbel, D. Ware and A. Bidani, *A human cardiopulmonary system model applied to the analysis of the Valsalva maneuver*, Am J Physiol, **281** (2001), H2661–79.
- [21] R. Mosteller, *Simplified calculation of body surface area*, N Engl J Med, **317** (1987), 1098.
- [22] R. Mukkamala, A. Reisner, H. Hojman, R. Mark and R. Cohen, *Continuous cardiac output monitoring by peripheral blood pressure waveform analysis*, IEEE Trans Biomed Eng, **53** (2006), 459–67.
- [23] M. Neal and J. Bassingthwaighe, *Subject-specific model estimation of cardiac output and blood volume during hemorrhage*, J Cardiovasc Eng, **7** (2007), 97–120.
- [24] J. Nelder and R. Mead, *A simplex method for function minimization*, Comput J, **7** (1965), 308–13.
- [25] D. Newell and R. Aaslid, “Transcranial Doppler,” Raven Press, New York, NY 1992.
- [26] V. Novak, P. Novak and R. Schonendorf, *Accuracy of beat-to-beat noninvasive measurement of finger arterial pressure using the Finapres: a spectral analysis approach*, J Clin Monit, **10** (1994), 118–26.
- [27] J. Olansen, J. Clark, D. Khoury, F. Ghorbel and A. Bidani, *A closed-loop model of the canine cardiovascular system that includes ventricular interaction*, Comp Biomed Res, **33** (2000), 260–95.
- [28] M. S. Olufsen, J. T. Ottesen, H. T. Tran, L. M. Ellwein, L. A. Lipsitz and V. Novak, *Blood pressure and blood flow variation during postural change from sitting to standing: model development and validation*, J Appl Physiol, **99** (2005), 1523–37.
- [29] M. S. Olufsen, H. T. Tran and J. T. Ottesen, *Modeling cerebral blood flow during posture change from sitting to standing*, J Cardiovasc Eng, **4** (2004), 47–58.
- [30] J. T. Ottesen and M. Danielsen, *Modeling ventricular contraction with heart rate changes*, J Theo Biol, **22** (2003), 337–46.
- [31] J. T. Ottesen, M. S. Olufsen and J. Larsen, “Applied Mathematical Models in Human Physiology,” SIAM, Philadelphia, PA, 2004.
- [32] R. Panerai, H. Coughtrey, J. Rennie and D. Evans, *A model of the instantaneous pressure-velocity relationships of the neonatal circulation*, Physiol Meas, **14** (1993), 411–18.
- [33] T. Parlikar, T. Heldt, G. Ranade and G. Verghese, *Model-based estimation of cardiac output and total peripheral resistance*, Comp Cardiol, **34** (2007), 379–82.
- [34] L. Pourcelot, *Applications cliniques de l’examen Doppler transcutane*, Coloques de l’Inst Natl Sante Rech Med, **34** (1974), 213–40.
- [35] B. Reading and B. Freeman, *Simple formula for the surface area of the body and a simple model for anthropometry*, Clin Anat, **18** (2005), 126–30.
- [36] V. Rideout “Mathematical and Computer Modeling of Physiological Systems,” Prentice Hall, Englewood Cliffs, NJ, 1991.
- [37] W. Shoemaker, *Fluids and electrolytes in the acutely ill adult*, in “Textbook of Critical Care” (eds. W. Shoemaker S. Ayres, A. Grenvik, P. Holbrook and W. Leigh Thompson), W. B. Saunders, Philadelphia, 1989.
- [38] J. Smith and J. Kampine, “Circulatory Physiology, the Essentials,” Williams and Wilkins, Baltimore, MD, 1990.

- [39] M. Velez-Reyes, “Decomposed Algorithms for Parameter Estimation,” Ph.D. Thesis, MIT, Cambridge, MA, 1992.
- [40] C. Vlachopoulos and M. O’Rourke *Diastolic prssure, systolic pressure, or pulse pressure* Curr Hyperten Rep, **2**(2000), 271–79.
- [41] K. Wesseling, J. Jansen, J. Settels and J. Screuder *Computation of aortic flow from pressure in humans using a nonlinear three-element model*, J Appl Physiol, **74** (1993), 2566–73.

Received July 24, 2008; Accepted September 24, 2008.

E-mail address: msolufse@math.ncsu.edu